

# An AAV Vector for Inducible Gene Expression Preferentially in Muscles

Yicong Le<sup>1</sup>, Zhengyun Jiang<sup>2</sup>, Xi Zheng<sup>3</sup>, Christina Marinaro<sup>4</sup>, Suzie Chen<sup>5</sup>, Bing Wang<sup>6</sup>, Suqing Zhao<sup>7</sup>, Min Chen<sup>8</sup>, Philip Furmanski<sup>9</sup>, Kun Zhang<sup>10</sup>, Renping Zhou<sup>11,\*</sup>

## Abstract

*Adeno associated viral (AAV) vectors has been used widely in gene therapy and efforts have been made to improve their utility by adding genetic elements that would enable targeting transgene expression to particular cells or tissues of interest and permitting on/off regulation of expression. In this study, we designed a recombinant AAV9 variant PHP.eB vector with muscle creatine kinase (Mck)-derived enhancers, a synthetic muscle-expression promoter, in combination with a third-generation tetracycline-inducible promoter, to drive expression of reporter genes luciferase and GFP (PHP.eB- $P_{mus}$ -TetOn-teLuc and PHP.eB- $P_{mus}$ -TetOn-eGFP, respectively). This recombinant vector expresses genes at high levels preferentially in muscle cells, that can be controlled by doxycycline (Dox) exposure both in vitro and in vivo. To test inducibility of these vectors in vivo, adult SKH hairless mice were injected intravenously with  $2 \times 10^{12}$  virus genomes. Dox-containing food (625 mg/kg) was given 1 day after virus injection to initiate expression. After one month, tissue luciferase activity was assayed. Luciferase expression level per viral genome in muscle tissues including biceps brachii, biceps femoris, and heart tissue were higher in  $P_{mus}$ -TetOn group. Long-term expression was also assessed for the PHP.eB- $P_{mus}$ -TetOn-teLuc vector: two weeks after virus injection and Dox induction, Dox-containing food was replaced with conventional diet and luciferase expression was tracked biweekly using IVIS in vivo imaging. Following Dox removal, luciferase expression decreased and by 6 weeks had returned to basal levels. Re-exposure to Dox stimulated luciferase expression to levels similar to the first Dox-induced expression. Removal of the second Dox stimulus resulted in slow loss of luciferase activity, which could again be re-induced by Dox exposure. These experiments indicate that this inducible, tissue-selective expression could be maintained in vivo for at least 18 weeks.*

## \*Author for Correspondence

Renping Zhou  
E-mail: rzhou@pharmacy.rutgers.edu

<sup>1,3,4</sup>Researcher, Department of Chemical Biology, Ernest Mario School of Pharmacy, Rutgers, The State University of New Jersey, Piscataway, NJ 08854, USA

<sup>2</sup>Researcher, School of Biomedical and Pharmaceutical Science, Guangdong University of Technology, Guangzhou, China

<sup>5,9</sup>Researcher, Department of Chemical Biology, Ernest Mario School of Pharmacy, Rutgers, The State University of New Jersey, Piscataway, NJ 08854, USA; Rutgers Cancer Institute of New Jersey, New Brunswick, NJ 08903, USA

<sup>6</sup>Researcher, Department of Medicine, University of Pittsburgh, Pittsburgh, PA 15261, USA

<sup>7,8,10</sup>Researcher, School of Biomedical and Pharmaceutical Science, Guangdong University of Technology, Guangzhou, China; School of Biotechnology and Health Science, Wuyi University, Jiangmen, China

<sup>11</sup>Associate Dean for Research, Professor, Department of Chemical Biology, Ernest Mario School of Pharmacy, Rutgers, The State University of New Jersey, Piscataway, NJ 08854, USA

Received Date: October 04, 2023

Accepted Date: November 01, 2023

Published Date: December 01, 2023

**Citation:** Yicong Le, Zhengyun Jiang, Xi Zheng, Christina Marinaro, Suzie Chen, Bing Wang, Suqing Zhao, Min Chen, Philip Furmanski, Kun Zhang, Renping Zhou. An AAV Vector for Inducible Gene Expression Preferentially in Muscles. International Journal of Genetic Modifications and Recombinations. 2023;1(2): 46–61p.

**Keywords:** Gene therapy, AAV, muscle specific promoter, Tet-on, inducible gene expression

## INTRODUCTION

Gene therapy is a promising approach for treating many diseases. An important consideration in the eventual application of many of the gene therapies in patients is restricting expression to particular cells and tissues involved in disease pathogenesis [1–3]. Tissue specific (or selective) expression would likely reduce off-target effects, minimize immunological attack of transduced cells and might enable use of lower doses/titer of the therapeutic vectors. In addition to spatial control, temporal control of transgene expression is desirable to

moderate expression time and levels, which can be of value in certain therapeutic situations, and which may also further improve the safety of gene therapies. Our interest is in development of new gene therapy approaches for several chronic neuromuscular diseases for the delivery of potential therapeutic genes including neurotrophic factors. It has been shown that inappropriate expression of some neurotrophic factors at too high levels or in the wrong time or place could have deleterious effects. For example, prolonged AAV-mediated ciliary neurotrophic factor (CNTF) expression in the retina for the treatment of retinitis pigmentosa resulted in functional loss [4–6]. Prolonged expression of glial cell line-derived neurotrophic factor (GDNF) in the treatment of Parkinson's disease also resulted undesirable side effects including aberrant axon sprouting, downregulation of tyrosine hydroxylase and weight loss [7–10]. In addition, some of the trophic factor receptors are known oncogenes, and uncontrolled ligand expression may result in tumorigenesis [11]. In this context we have sought to design vectors for gene delivery to target muscle cells for promoting motor neuron survival that enable both spatial and temporal control of gene expression over extended periods of time *in vivo*. Prior studies by others have sought to achieve selective muscle expression using vectors built on AAV serotypes that exhibit a muscle-selective tropism [12]. Others have modified AAV vectors expressing genes of interest under the control of strong muscle-specific promoters [1, 13, 14]. However, there are no reports to date of an AAV vector demonstrating sustained muscle expression together with temporal control *in vitro* and *in vivo*.

Several approaches have been used to achieve gene expression controls both spatially and temporally. One approach is to generate inducible expression using a tissue or cell type-specific promoter. For example, Stieger et al. designed regulatable AAV vectors using retinal pigmented epithelium (RPE) 65 gene promoter to drive the expression of the reverse tetracycline-dependent transactivator (rtTA) which in turn initiates transcription of the gene of interest placed downstream of the tetracycline-responsive promoter for gene expression in the retina. They demonstrated specific expression in the RPE only after induction with doxycycline and the expression can be induced repeatedly over 2.5 years [15]. Similar approaches have been used since to design spatially and temporally controlled gene expression using AAV vectors in the liver with the liver promoter albumin [16] and brain using the neuron-specific synapsin promoter [17, 18]. New innovative approaches have also been developed recently to control gene expression temporally using riboswitch, a ribozyme controlled by small molecules [19]. In the presence of the inducing compound, the included ribozyme is inactivated (or activated) to cleave target mRNA allowing on/off switch of target gene expression. Another interesting method is to regulate gene expression by regulating splicing using small compounds. Monteyes et al. took advantage of available drugs for spinal muscular atrophy that promote splicing of the SMN pseudogene SMN2 to complement functional loss of SMN1 [20], and designed expression cassettes controlled by drug-induced splicing. While these new methods are very exciting innovations, they are still at the early stages of therapeutic applications. The levels of induction by the riboswitches also tend to be modest [19], and tissue or cell-type specific applications are yet to be developed. Thus, we opted to develop a spatially and temporally controllable muscle gene vector using a well-characterized muscle promoter and the rtTA inducible system.

Here we report the generation of a recombinant AAV gene delivery vector with both spatial and temporal gene expression controls. The vector contains a rtTA expressed by a muscle promoter and Tet promoter controlled by doxycycline for the expression of gene of interest. In addition, we tested several different AAV serotypes and found an AAV9 variant, PHP.eB [21], is highly specific for muscle gene delivery. We show that these vectors provide regulatable spatial and temporal gene expression *in vitro* and *in vivo*.

## MATERIALS AND METHODS

### Recombinant AAV Vectors

AAV- $P_{CMV}$ -eGFP was purchased from Addgene (Cat. #67634) [22]. AAV- $P_{CMV}$ -teLuc was generated by substituting the eGFP gene with a teLuc gene PCR fragment, utilizing pcDNA3-teLuc c-myc (Addgene Cat. 100026) [23] as the template. This replacement was done using Takara Bio In-Fusion cloning kit (Cat. 638956). To construct AAV- $P_{mus}$ -TetOn vectors, a DNA fragment containing XhoI-

transcription blocker sequences - two copies of the Mck enhancer element-C5-12 synthetic promoter [24]-XbaI, was synthesized (Genscript Biotech Corp, NJ) and then used to replace the XhoI-XbaI fragment containing the transcription blocker and hPGK promoter in pAAVpro-Tet-One plasmid (Takara Bio Cat. #634311), generating pAAV-P<sub>mus</sub>-TetOn. pAAV-P<sub>mus</sub>-TetOn-eGFP was constructed by ligating the EcoRI-NotI eGFP DNA fragment from pEGFP-N1 plasmid (Clontech Cat. #6085-1; Genbank accession # U55762.1) into the EcoRI-NotI sites of the pAAV-P<sub>mus</sub>-TetOn plasmid. pAAV-P<sub>mus</sub>-TetOn-teLuc was constructed by ligating a PCR teLuc fragment using pcDNA3-teLuc c-myc plasmid as a template into the NheI-BamHI sites of pAAV-P<sub>mus</sub>-TetOn downstream of the TRE3GS promoter. In addition, a chimeric intron from pCI-Neo plasmid (Promega, Cat. #E1841; Genbank Accession # U47120) was inserted between the TRE3GS promoter and teLuc gene to enhance expression [10, 11].

### Cell Culture

HEK293T cells (Takara Bio) were cultured in growth medium composed of DMEM (4500mg/L Glucose, Gibco) supplemented with 10% FBS (Gibco), 1x MEM non-essential amino acid (MEM NEAA, Gibco), 1mM Sodium Pyruvate, 100U/mL penicillin-streptomycin (Gibco), and 1.5 g/L Sodium Bicarbonate. C2C12 muscle cells were maintained in DMEM (4500mg/L Glucose, Gibco) supplemented with 10% FBS, and differentiated in DMEM (4500mg/L Glucose, Gibco) supplemented with 2% horse serum. C2C12 myotubes were infected at differentiation day 4. For cells infected with AAV-P<sub>mus</sub>-TetOn-eGFP/teLuc, the tissue culture medium was supplemented with 1 µg/mL doxycycline.

### Virus Production and Purification

AAVs were produced and purified based on published protocol [13]. In brief, 70%-80% confluence LentiX-293T cells (Takara Bio) in growth medium (described above) were transfected with recombinant pAAV, pHelper (Takara Bio #6234), and pUCmini-iCap-PHP.eB [21]/AAV2-MTP [12]/ pDGM6 (Addgene #110660) for PHP.eB, 2-MTP and 6 capsid, respectively. At day (D)1 and D3 post transfection, medium was refreshed with growth medium containing 4% FBS, replaced D3 medium were kept in 4°C until later process. At day 5 post transfection, the medium (together with D3 medium) and cells were collected and processed separately. Cells were lysed through 4-6 freeze and thaw cycles; the cell lysate was then centrifuged at 20,000xg for 30 minutes, and the supernatant was collected for virus purification. Viral particles in the culture medium were precipitated out polyethylene glycol (PEG) 8000 solution (8% PEG and 0.5M NaCl final concentration) and centrifuged at 5,000xg for 1 hour at 4°C. Concentrated AAVs were purified by two rounds of CsCl gradient ultracentrifugation (38,000 rpm, 16 hr, 20°C). For smaller scale AAV production, viruses were collected by the AAVpro Extraction Kit (Takara Bio) for *in vitro* use. Virus titers were determined by qPCR with the following primers:

eGFP+: 5'-AAGCTGACCCTGAAGTTCATCTGC-3';  
eGFP-: 5'-CTTGTAAGTGGCCGTCGTCCTTGAA-3';  
teLuc+: 5'-CCGGCTACAACCTTGAGTCAAGTCC-3';  
teLuc-: 5'-CTTCATACGGGATGATGACATGGATGTC-3'.

### Luciferase Assay and Genomic DNA Extraction

Cells were lysed in NP-40 buffer (1% NP-40, 150 mM NaCl, and 50 mM Tris-Cl, pH8) supplemented with 1% (v/v) Proteinase Inhibitor Cocktail (Sigma P8340) for 30 minutes on ice, supernatants were collected after centrifuge at 1,800g for 20 minutes.

Tissues were homogenized and then lysed using the buffer described above. After centrifugation, the supernatants were used for luciferase assay and the pellets were saved for genomic DNA extraction with the Monarch Genomic DNA Extraction Kit (NEB). Gene copy number were analyzed by qPCR and quantified via a standard curve and then normalized by total DNA concentration of the sample.

Diphenylterazine (DTZ) were used as luciferase substrate. DTZ was prepared by dissolving it in an *in vivo* luciferase assay buffer composed of 8% glycerol (v/v), 10% ethanol (v/v), 10% Hydroxypropyl-β-cyclodextrin (m/v), 35% PEG 400 (v/v), and water to achieve a concentration of 2.5 mg/mL. For *in vitro* assays, the DTZ solution was further diluted in the *in vitro* luciferase buffer, which consisted of 1

mM Cyclohexanediaminetetraacetic acid (CDTA), 0.5% Tergitol NP-40, 0.05% antifoam 204, 150 mM KCl, 100 mM MES (pH 6.0), and 35 mM thiourea. To conduct bioluminescence measurements in 96-well plates, 20  $\mu$ L of cell or tissue lysates were mixed with 100  $\mu$ L of DTZ in the *in vitro* buffer. Each sample was analyzed in triplicate.

## Animals

The animal study protocol was approved by the Institutional Review Board (or Ethics Committee) of Rutgers, the State University of New Jersey (protocol code PROTO201702492).

For optimal *in vivo* imaging system (IVIS) imaging, mouse hair needs to be removed, however, it is harmful to the animals if the process is done repeatedly. Thus, the SKH hairless mice were used for safe and easy imaging.  $2 \times 10^{12}$  AAV vg/animal in PBS were injected retro-orbitally following ketamine/xylazine anesthesia. If gene expression induction is needed, 625 mg/kg Dox diet (Envigo) were provided. Mice were anesthetized by isoflurane inhalation. 100  $\mu$ L DTZ *in vivo* solution (2.5 mg/mL) were injected subcutaneously 5 minutes before imaging. Images were taken with IVIS Spectrum, PerkinElmer Co., Ltd. The exposure time was 2 minutes.

Animals were sacrificed before tissue dissection. Tissues were lysed in NP-40 buffer for luciferase assay as described above. Tissue genomic and viral DNA were extracted by Monarch Genomic DNA Extraction Kit (New England Biolabs) per manufacture's instruction. DNA concentrations were measured using NanoDrop 2000 (Thermo Fisher). Tissue viral genome copy number were determined by qPCR.

## RESULTS

### Effect of AAV Serotype on Preferential Targeting of Muscle Cells

The main objective of this study is to design a good approach to express genes in the muscle cells. We first assessed several AAV capsids which have been reported to have high efficiency for muscle infection to identify a capsid that has high specificity for muscle cells. AAV serotype 2 (AAV2) is the initial serotype isolated and has been used extensively in AAV-based gene therapy studies [25]. AAV2 can infect several tissues, including the cells of central nervous system (CNS), liver, muscle, and lung [12, 26-30]. AAV2 muscle tropism is increased with insertion of a 7 amino acid muscle-targeting peptide into the capsid (AAV2-MTP) [12]. AAV6 exhibits a higher transduction rate in skeletal muscle cells [31, 32]. In addition, we also tested PHP.eB, a variant of AAV9 which has been shown to target liver, heart, skeletal muscles, and CNS more efficiently [33, 34]. Thus, we chose to test AAV2-MTP, AAV6 and PHP.eB *in vitro* to assess their ability to preferentially infect muscle cells.

HEK293T and differentiated C2C12 muscle cells were infected with the same number of virus genomes per cell (MOI 25) of AAV2-MTP- $P_{CMV}$ -eGFP, AAV6- $P_{CMV}$ -eGFP, and PHP.eB- $P_{CMV}$ -eGFP. Expression levels were assessed based on the intensity of GFP fluorescence (Figure 1). In differentiated C2C12 muscle cells, all three vectors exhibited similar GFP expression levels. Notably, AAV6 displayed significantly higher expression levels in HEK293T cells compared to its expression in differentiated C2C12 muscle cells. AAV2-MTP had lower expression level in HEK293T cells than AAV6 but showed no preference for the muscle cells. PHP.eB showed the greatest differential GFP expression in C2C12 versus HEK293T cells and was thus used for further studies.

(A) HEK293T and differentiated C2C12 muscle cells were infected with AAV2-MTP- $P_{CMV}$ -eGFP, AAV6- $P_{CMV}$ -eGFP, and PHP.eB- $P_{CMV}$ -eGFP. HEK293T and C2C12 cells were cultured in 6-well plates and subsequently infected with each virus vector at a multiplicity of infection (MOI) of 25. Images of HEK293T cells were captured 3 days after viral infection, while images of C2C12 muscle cells were acquired 5 days post-infection. All images were taken under same magnification and exposure settings, with scale bars indicating 200  $\mu$ m. (B) Analysis of GFP expression was performed, and fluorescence intensity was quantified using Image J. The intensity measurements presented here represent the average of measurements from three separate wells. *P*-values were computed using Student's t-test. \*\*  $p < 0.01$ ; \*\*\*\*  $p < 0.0001$ .

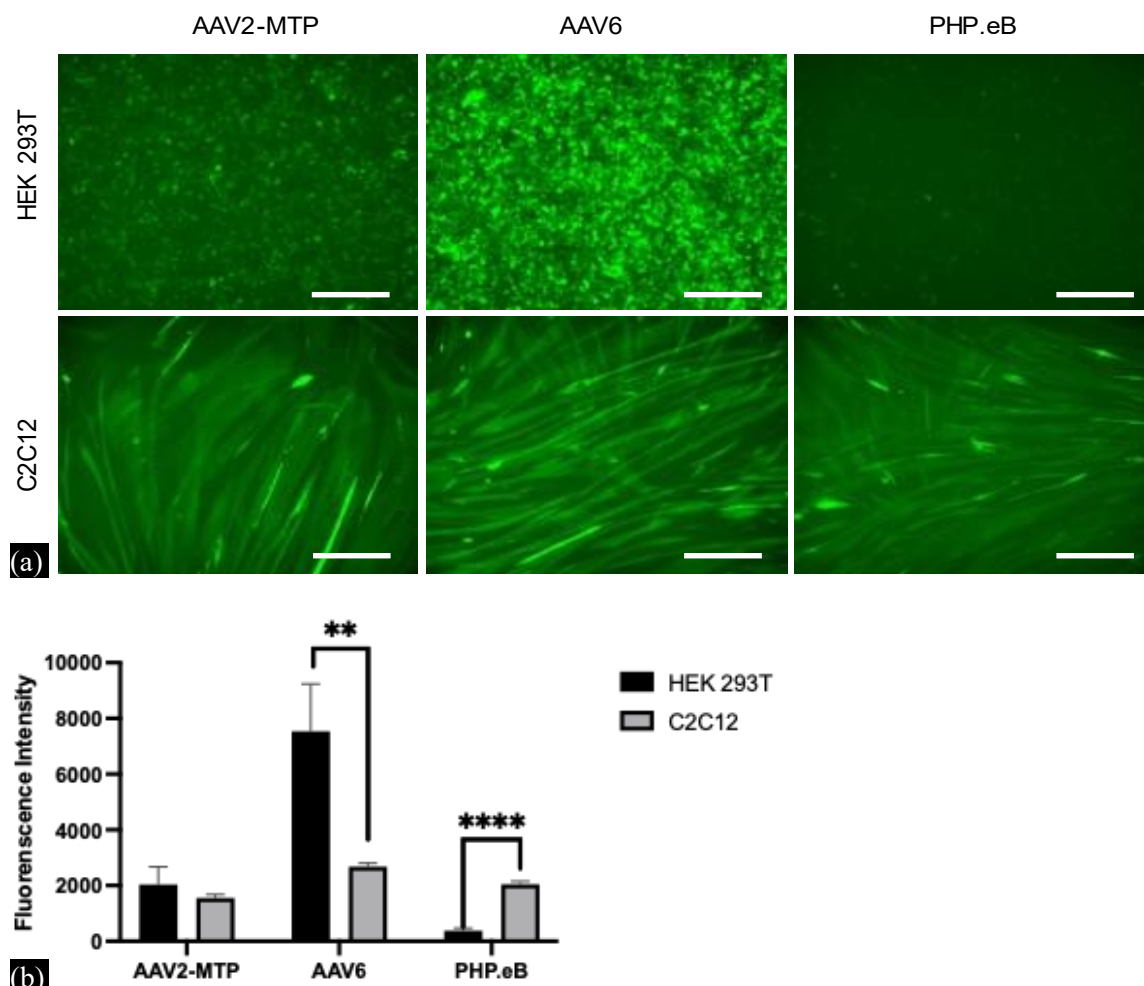


**Figure 1.** (a, b) Muscle cell preference of AAV2-MTP, AAV6, and PHP.eB.

### Design and Construction of Spatially and Temporally Regulatable Vectors for Gene Delivery in Muscle Cells

In the development of a gene delivery vector that allows spatial and temporal regulation, we opted to employ the hybrid muscle promoter  $P_{mus}$ . This promoter was chosen to control the expression of the tetracycline-controlled transcriptional activator TetOn3G, which, in turn, facilitates the transcription of the gene of interest in a muscle cell-specific manner. This regulation is achieved through the utilization of a tetracycline response element promoter PTRE3GS, comprising seven tetracycline operator (TetO) sequences and a CMV minimal promoter, contingent upon the presence of Doxycycline (Dox) (Figure 2A). Notably, PTRE3GS was a modified iteration of the original PTRE, engineered to eliminate binding sites for endogenous mammalian transcription factors, thereby reducing background expression [35]. For this study, we used eGFP and teLuc (a modified nano-luciferase with red-shifted high bioluminescence) as reporter genes [23]; the constructs are designated PHP.eB- $P_{mus}$ -TetOn-eGFP and PHP.eB- $P_{mus}$ -TetOn-teLuc, respectively. Genomic fidelity of the construct was confirmed through restriction enzyme digestion and sequencing.

HEK 293T and C2C12 cells were cultured in 12-well plates and infected same amount (MOI 3000) of different viral vectors. (A) Map of the muscle-targeting regulatable recombinant PHP.eB vector. ITR, inverted terminal repeat; SV40, simian virus 40 promoter; TetOn3G: 3<sup>rd</sup> generation tetracycline-controlled transcriptional activator;  $P_{mus}$ : muscle-expression promoter; A: poly-adenylation signal; P: transcription pause signal of the human  $\alpha 2$  globin gene; Dox, doxycycline;  $P_{TRE3GS}$ , third-generation tet-responsive promoter; teLuc, a modified nanoluciferase. (B) GFP expression from the muscle-

targeting regulatable vector and CMV control vector. Scale bars are 200  $\mu\text{m}$ . (C) teLuc activity assay. AU/ $\mu\text{g}$ , arbitrary unit per microgram of protein. Each measurement represents the mean  $\pm$  SD value of triplicate wells. The  $p$ -value was determined using Student's  $t$ -Test; \*\*\* $P < 0.001$ .

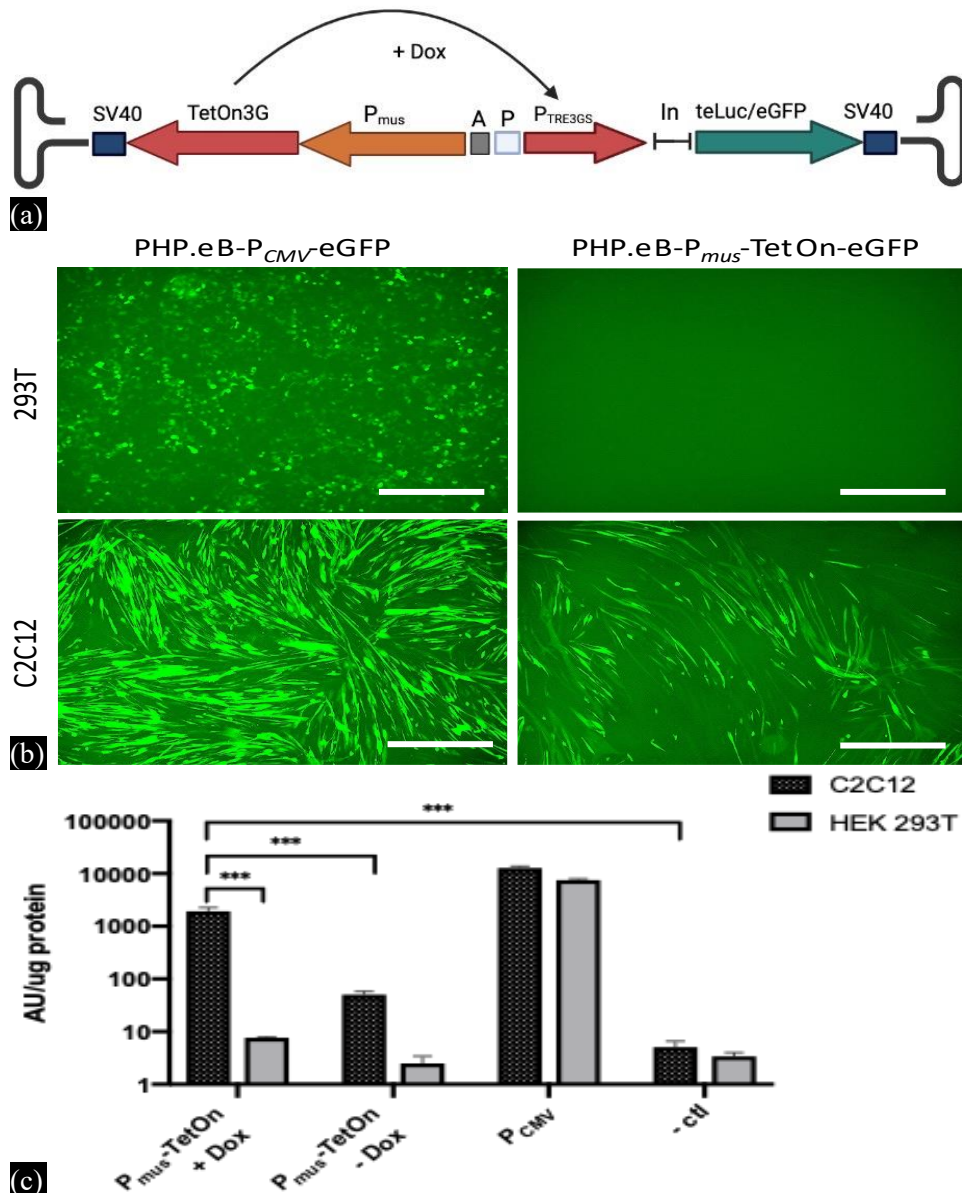


**Figure 2.** (a–c) Muscle gene delivery vector design and testing in vitro.

### Test of Recombinant Muscle AAV Vectors *In vitro*

PHP.eB-P<sub>mus</sub>-TetOn-eGFP and PHP.eB-P<sub>mus</sub>-TetOn-teLuc viruses were prepared using the 3 plasmids co-transfection method in HEK293T cells. PHP.eB-P<sub>CMV</sub>-eGFP/teLuc virus was used as a constitutive expression control. The same MOI (3000) of PHP.eB-P<sub>mus</sub>-TetOn-eGFP/teLuc and PHP.eB-P<sub>CMV</sub>-eGFP/teLuc viruses was used to infect HEK293T and differentiated C2C12 muscle cells. Dox (1  $\mu\text{g}/\text{mL}$ ) was added to the medium at day 1 post-infection for the P<sub>mus</sub>-TetOn groups. At day 3 post-infection, images were taken for GFP expression (Figure 2B), and cells were lysed for luciferase activity assay for the respective reporter gene vectors.

PHP.eB-P<sub>CMV</sub>-eGFP exhibited high levels of expressions in both HEK293T and C2C12 muscle cells, whereas PHP.eB-P<sub>mus</sub>-TetOn-eGFP showed little to no expression in HEK293T cells but moderate eGFP

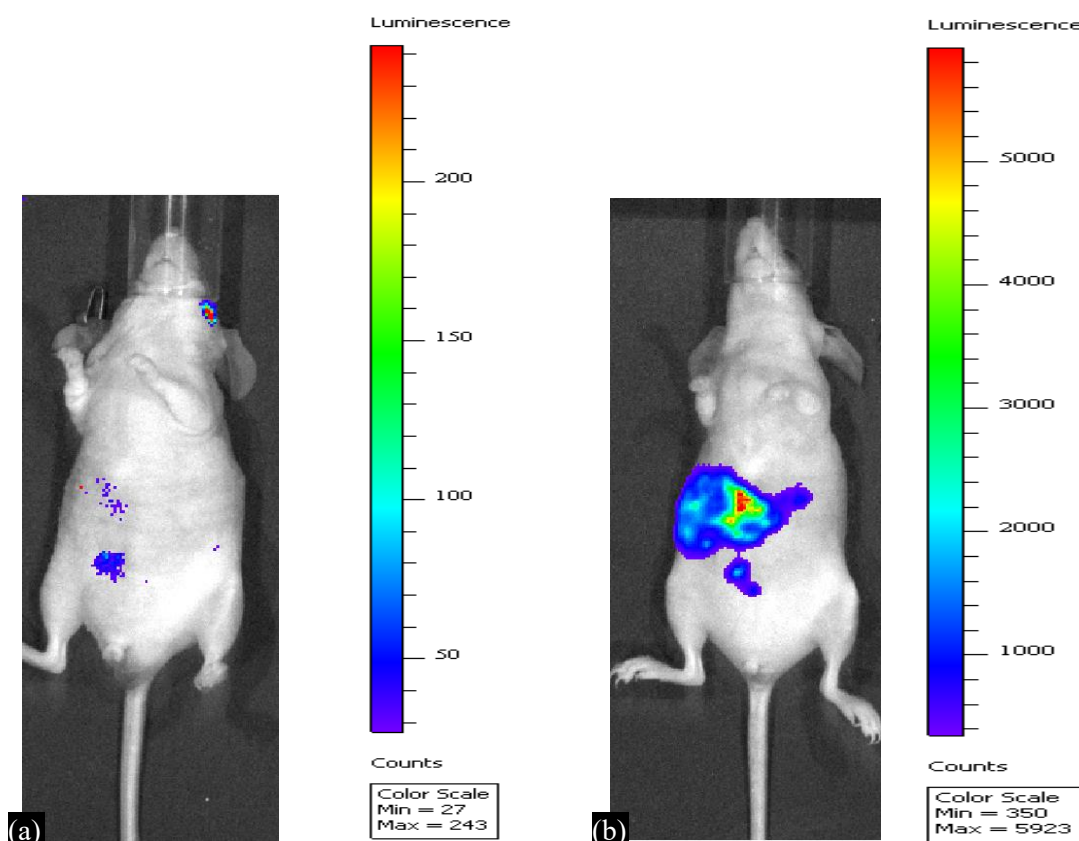


expression in differentiated C2C12 muscle cells in the presence of Dox (Figure 2B). To assess the levels of reporter gene expression in different cell lines, we performed luciferase activity assays on cell extracts following the infection of PHP.eB- $P_{CMV}$ -teLuc and PHP.eB- $P_{mus}$ -TetOn-teLuc (Figure 2C). In the  $P_{mus}$ -TetOn group, where Dox was applied, luciferase activity was observed to be 250-fold greater in differentiated C2C12 muscle cells when compared to HEK293T cells. In C2C12 muscle cells, with the presence of Dox, the luciferase activity was 38-fold higher than without Dox induction. These results indicate that the PHP.eB- $P_{mus}$ -TetOn vector can preferentially express reporter genes in muscle cells and the expression can be regulated by Dox administration.

Adult mice received a retro-orbital injection of viruses at a concentration of  $1 \times 10^{14}$  vector genomes per kilogram (vg/kg). In vivo imaging was conducted using an imaging system (IVIS) one month after the viral injection, with the administration of Diphenylterazine (DTZ) occurring 5 minutes prior to imaging. The results are as follows: (A) Mice injected with PHP.eB- $P_{mus}$ -TetOn-teLuc without Dox induction, (B) Mice injected with PHP.eB- $P_{mus}$ -TetOn-teLuc with Dox induction, and (C) The average luminescence values from IVIS images obtained from different animals ( $n=3$ ) under both Dox-induced and non-induced conditions.  $p$ -value was determined using two-tailed  $t$ -test. \*  $p < 0.05$ .

### Test of Recombinant Muscle AAV Vectors *In vivo*

SKH hairless mice were injected intravenously with  $2 \times 10^{12}$  PHP.eB- $P_{CMV}$ -teLuc or PHP.eB- $P_{mus}$ -TetOn-teLuc viral vector particles and randomly divided into three groups:  $P_{CMV}$  (Figure S1);  $P_{mus}$ -TetOn + Dox, fed the Dox-containing diet starting at 2 days post-virus injection;  $P_{mus}$ -TetOn - Dox, fed only conventional diet. One month following the virus injection, whole body imaging was conducted using the IVIS *in vivo* imaging system to assess the level of luciferase expression (Figure 3). In the presence of Dox (Figure 3B), the bioluminescence level was approximately 25-fold greater compared to the group without Dox induction (Figure 3A). This result suggested that the  $P_{mus}$ -TetOn system is capable of gene of interest expression *in vivo* and this expression can be controlled by the administration of Dox.



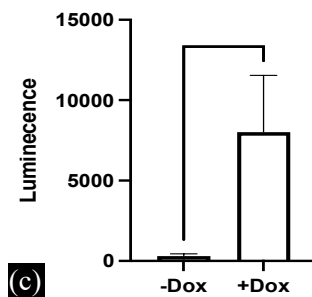


**Figure 3.** (a–b) Bioluminescence Imaging of Hairless Mice after retro-orbital Viral Injection.

To further examine the tissue distribution of reporter gene expression, mice were sacrificed one month post virus injection and luciferase activity measured in tissue extracts. In the PHP.eB- $P_{CMV}$ -teLuc group, the highest expression levels were found in diaphragm and heart, brain had a moderate expression level and muscle tissue expression levels were lower compared to other tissues (Figure S2A). In the  $P_{mus}$ -TetOn +Dox group, the highest expression levels were found in heart, skeletal muscles, and brain. The liver had less reporter gene expression, and kidney tissue luciferase expression was not detectable (Figure 4B). In the absence of Dox induction, small amount of activity was detected in all tissues tested but at 10 to 20-fold lower levels than in the presence of Dox, with the exception of heart, where high levels of activity were detected without Dox induction, but still 5-fold less than with Dox treatment.

We also measured viral genomic DNA content in the tissue extracts. Viral copy number was detected by qPCR and then normalized to genomic DNA concentration. The results are shown in Figure 4C. Liver and brain, which are the two main targets for PHP.eB, showed high amount of virus DNA. Other tissues showed detectable virus DNA, at lower levels than liver and brain. In every tissue, the amount of virus DNA was the same in Dox treated and untreated mice.

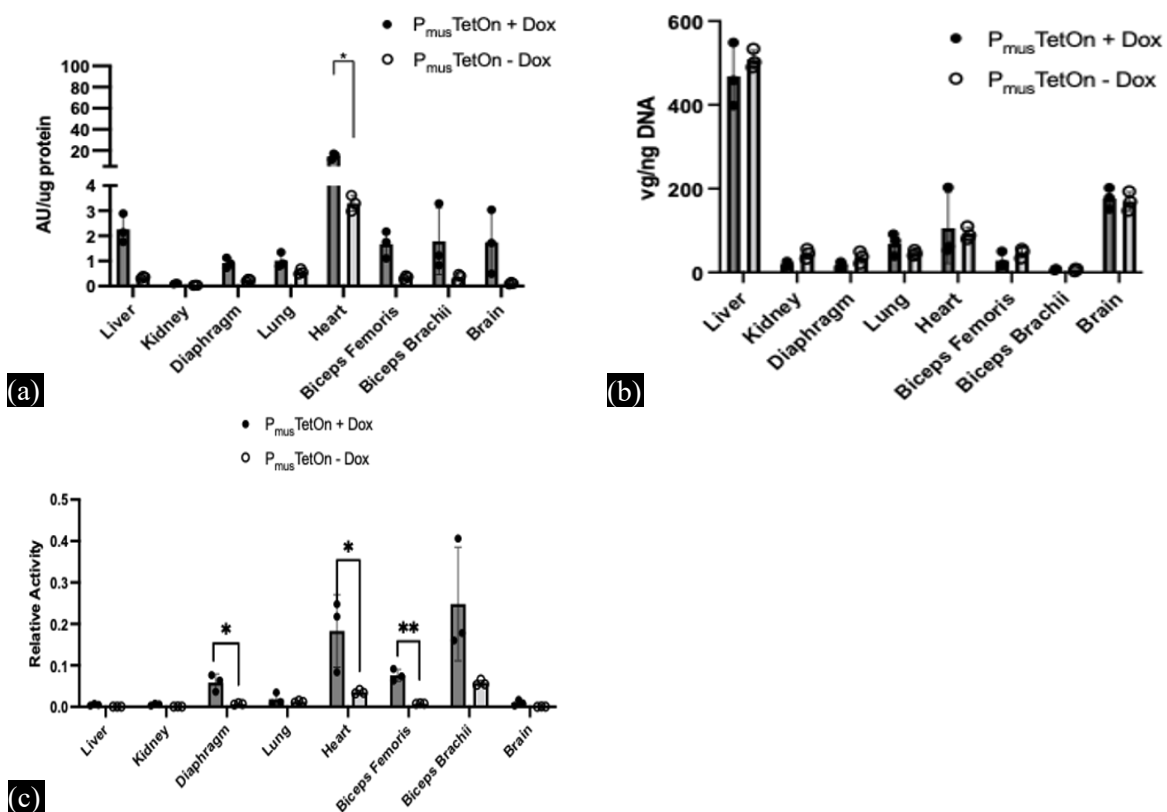


**Figure 4.** (a–c) Tissue analysis of luciferase activity induced by AAV Vectors.



Additionally, we conducted an analysis of reporter gene expression in relation to the gene copy number present in the examined tissues. The relative expression level was determined by dividing the tissue luciferase enzymatic activity by the viral genome copy number (normalized by genomic DNA concentration) within the corresponding tissue extract. Based on this parameter, the highest relative reporter expression levels were observed in heart and diaphragm in the  $P_{CMV}$  groups (Supplementary Figure 2C), and biceps brachii and heart in  $P_{mus}$ -TetOn + Dox group (Figure 4C).

One month post viral injection and Dox induction, heart, lung, diaphragm, liver, kidney, biceps femoris, biceps brachii muscles, and brain tissues were harvested from three animals in each group for analysis. (A) Tissue samples from PHP.eB- $P_{mus}$ -TetOn-teLuc injections, both with and without Dox induction, were subjected to luciferase activity assays using the DTZ substrate. The results are presented as mean  $\pm$  standard deviation (SD). (B) The virus gene copy numbers were determined via qPCR analysis, and the data are presented as mean  $\pm$  SD. (C) The virus gene's relative activity within animal tissues following PHP.eB- $P_{mus}$ -TetOn-teLuc injection, with and without Dox induction, was computed. These relative activities were obtained by normalizing the bioluminescence measured in the tissue luciferase assay to the viral genome copy number within the same tissue specimen. All samples were tested in triplicate.  $p$ -values were determined using Student's  $t$ -Test. \*  $p < 0.05$ ; \*\*  $p < 0.01$ .

### Long-term Gene Expression and Repeat Induction *In vivo* by the Recombinant AAV Vectors

To assess persistence of transgene expression and its sustained regulation by Dox, PHP.eB- $P_{mus}$ -TetOn-teLuc ( $2 \times 10^{12}$  vg/animal) viruses were injected intravenously (i.v.) into hairless mice via retro-orbital route ( $n=3$ ). Following the virus injection and the initiation of Dox induction, *in vivo* luciferase activity was continuously monitored using IVIS. This monitoring commenced two weeks after the induction began, with baseline expression being captured one day after the virus injection, prior to the administration of Dox-containing food. Subsequently, Dox was discontinued, and the expression of luciferase was tracked every two weeks thereafter. In the absence of Dox, reporter expression returned to basal level at 6 weeks post-injection (Figure 5). At that point, Dox-containing food was provided again. This second induction drove gene expression to level comparable to the first induction. A third cycle of Dox removal and re-induction showed the same pattern of luciferase expression.

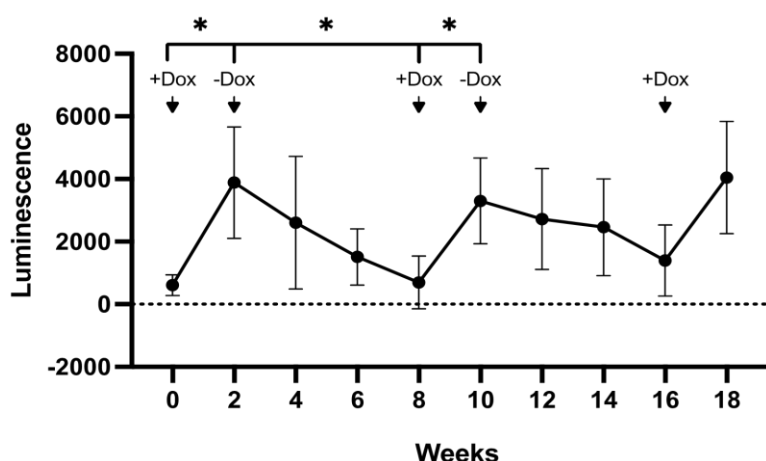


**Figure 5.** AAV9- $P_{mus}$ -TetOn-teLuc multiple induction.

$1 \times 10^{14}$  vg/kg viruses were injected intravenously into hairless mice ( $n=3$ ). Dox-containing food pellets were given for 2 weeks post injection and then removed until luciferase activity dropped to basal level (6 weeks). IVIS imaging were taken at the indicated time point, diphenylterazine (DTZ) was injected 5 minutes before imaging. Dox induction was tracked through 3 cycles of administration/withdrawal via IVIS and the luminescence values were plotted. Each data point represents the mean  $\pm$  SD value bioluminescence of 5 animals in each time point. The  $p$ -value was determined using Student's  $t$ -Test. \*  $p < 0.05$ .

## DISCUSSION

This study describes the development of an AAV vector that allows for control over gene expression *in vitro* and *in vivo*, both spatially and temporally. The basis of this construct is the use of  $P_{mus}$  hybrid enhancer/promoter to drive gene expression to high levels in muscle cells, and the use of the TetOn system to serve as a manipulatable expression switch.

AAV is widely used in gene therapy pre-clinical investigations and clinical trials because of its low cytotoxicity and immunogenicity [36, 37]. Several AAV gene therapy treatments are now used in the clinic for genetic diseases including spinal muscular atrophy [29] and Leber's congenital amaurosis [38]. AAV vectors have the capability to infect various species and tissues while typically eliciting only mild immune responses. [37]. Different AAV serotypes recognize distinct cell receptors and therefore display specific tissue tropism [25, 39]. AAV6 and AAV9 serotypes were previously reported to exhibit tropism for the skeletal muscle and heart tissues by different groups [40–43]. In addition, for better muscle tissue targeting, Xiao et. al. engineered into the AAV2 capsid a 7 amino acid muscle targeting peptide (MTP), and this modification enhanced tropism to various muscle tissues and particularly to the heart [12]. In this study, we similarly found that the AAV9 variant PHP.eB demonstrated the greatest selectivity for the muscle cells and tissues among the serotypes tested.

Another approach to achieve a high level of expression in the muscle tissues using recombinant AAV is to express the gene of interest under strong muscle promoters. The promoter and enhancer derived from human cytomegalovirus (CMV) have been recognized as among the most powerful DNA elements for inducing transgene expression in a wide range of mammalian cells [44, 45]. However, promiscuous, high-level gene expression can cause strong immune responses and undesired side effects [14, 46, 47]. We aimed to develop an AAV vector for muscle expression and eventual application to treatment of certain neuromuscular diseases. Wang et. al. modified a synthetic muscle promoter (C5-12) by adding a 206 bp Mck enhancer [48]. They reported that the addition of the Mck enhancer increased the expression of the synthetic promoter 2 to 3 times and allowed high expression in C2C12 myotubes as well as in mouse skeletal muscle, to even greater levels than the CMV promoter [48]. We used a comparable construct that incorporates two Mck enhancer elements positioned upstream of the synthetic muscle promoter. This combined with the TetOn system enabled us to achieve precise control over both the spatial and temporal aspects of gene expression.

The Tet inducible system has been used for transgene expression in different cells and tissues (e.g., human cancer cell lines, PC12 cells, neurons, and rodent retina) via the AAV vectors [49–52]. Efforts have also been made to use the AAV-Tet vectors to treat various diseases in animal models including breast cancer [53], ischemia [54], cochlear damage [55], Alzheimer Disease [56], and bone formation [57]. Gene silencing can also be achieved by Tet-controlled AAV vector to express shRNA [58] or gRNA in CRISPR system [59]. Moreover, a dual viral vector (Lentivirus and AAV) infection strategy has been used to express both TetOn and TetOff elements to trace different neurons in specific brain region [60]. A recent study reported that after locoregional intravenous injection, the AAV-Tet vector can be repeatedly induced by Dox for at least 5 years in monkey retina [61].

The combination of tissue-specific promoter and Tet-inducible element has also been tested in AAV in previous studies. Vanrell et. al. designed a recombinant AAV8 vector with the albumin promoter and a mutated reverse tetracycline transactivator (rtTAM2) to achieve liver-specific Tet-inducible gene expression [16]. Stieger et. al. tested the AAV vectors using the RPE65 promoter to drive expression of the TetOn element. The reporter gene expression can be repeat induced for over 2.5 years [15]. Dogbevia et.al. used a pan-neuronal specific promoter (hSYN) together with the tTA or rtTA element in AAV for injection into the cortex and hippocampus [17]. They showed that the reporter gene expression can be induced with (rtTA) or without Dox (tTA), and the induction of gene activation or deactivation can be repeated. Sohn et. al. designed a single AAV vector platform to use the hSYN promoter together with the TetOff element to achieve efficient labeling of central neurons in mouse brain [18].

In this study, we inserted the Mck enhancer/synthetic muscle promoter along with the TetOn3G system into the PHP.eB vector. This modified vector allows for enhanced expression of a target gene within C2C12 myotubes in comparison to HEK293T cells, and this expression can be triggered by the administration of Doxycycline. In our *in vivo* experiments, we observed a higher relative expression level in the muscles using the Mck-TetOn vector compared to the CMV vector. Additionally, we successfully demonstrated repeatable induction and a return to baseline expression levels through three cycles of Doxycycline administration and withdrawal, spanning a period of 18 weeks, which represents the longest duration tested.

Although we showed that the relative gene expression level is higher in biceps brachii and heart from the PHP.eB-P<sub>mus</sub>-TetOn-teLuc vectors, the injected viruses were mostly concentrated in the liver and brain tissue, which result in the high overall reporter gene expression in these two sites. It is well known that AAV vectors are predominantly sequestered in the liver after systemic injection [39, 62]. To minimize liver infection, it is possible to use AAV variant proteins containing liver-de-targeted mutations [63–65]. In addition, intramuscular injection can also be used to minimize off-target expression.

The vectors and strategies described may prove useful as a platform for developing gene therapy approaches for neuromuscular diseases in which spatial and temporal control of gene expression are goals, although further improvements are clearly needed.

## CONCLUSION

In this study, we generated a recombinant AAV vector based on the AAV9 variant PHP.eB which contains MCK derived enhancers, a synthetic muscle-expression promoter, and a third-generation tetracycline-inducible promoter. This AAV vector can express gene of interest preferentially in muscle cells and can be induced by the presence of Dox both *in vitro* and *in vivo*. After retro-orbital virus injection in the mice, the reporter gene expression can be turned on and off repeatedly by Dox-containing food, and the longest time tested for re-inducement was 18 weeks.

## Funding

This research was funded by the Garbe Chair and by Panamera, Inc NJ.

## REFERENCE

1. Aguti, S., A. Malerba, and H. Zhou, The progress of AAV-mediated gene therapy in neuromuscular disorders. *Expert Opin Biol Ther*, 2018. **18**(6): p. 681–693.
2. Chamberlain, J.R. and J.S. Chamberlain, Progress toward Gene Therapy for Duchenne Muscular Dystrophy. *Mol Ther*, 2017. **25**(5): p. 1125–1131.
3. Sudhakar, V. and R.M. Richardson, Gene Therapy for Neurodegenerative Diseases. *Neurotherapeutics*, 2019. **16**(1): p. 166–175.
4. Liang, F.Q., et al., Long-term protection of retinal structure but not function using RAAV.CNTF in animal models of retinitis pigmentosa. *Mol Ther*, 2001. **4**(5): p. 461–72.
5. Bok, D., et al., Effects of adeno-associated virus-vectored ciliary neurotrophic factor on retinal structure and function in mice with a P216L rds/peripherin mutation. *Exp Eye Res*, 2002. **74**(6): p. 719–35.
6. Schlichtenbrede, F.C., et al., Intraocular gene delivery of ciliary neurotrophic factor results in significant loss of retinal function in normal mice and in the Prph2Rd2/Rd2 model of retinal degeneration. *Gene Ther*, 2003. **10**(6): p. 523–7.
7. Georgievska, B., D. Kirik, and A. Bjorklund, Aberrant sprouting and downregulation of tyrosine hydroxylase in lesioned nigrostriatal dopamine neurons induced by long-lasting overexpression of glial cell line derived neurotrophic factor in the striatum by lentiviral gene transfer. *Exp Neurol*, 2002. **177**(2): p. 461–74.

8. Hovland, D.N., Jr., et al., Six-month continuous intraputamenal infusion toxicity study of recombinant methionyl human glial cell line-derived neurotrophic factor (r-metHuGDNF) in rhesus monkeys. *Toxicol Pathol*, 2007. **35**(7): p. 1013–29.
9. Manfredsson, F.P., et al., Nigrostriatal rAAV-mediated GDNF overexpression induces robust weight loss in a rat model of age-related obesity. *Mol Ther*, 2009. **17**(6): p. 980–91.
10. Su, X., et al., Safety evaluation of AAV2-GDNF gene transfer into the dopaminergic nigrostriatal pathway in aged and parkinsonian rhesus monkeys. *Hum Gene Ther*, 2009. **20**(12): p. 1627–40.
11. Coulier, F., et al., Human trk oncogenes activated by point mutation, in-frame deletion, and duplication of the tyrosine kinase domain. *Mol Cell Biol*, 1990. **10**(8): p. 4202–10.
12. Yu, C.Y., et al., A muscle-targeting peptide displayed on AAV2 improves muscle tropism on systemic delivery. *Gene Ther*, 2009. **16**(8): p. 953–62.
13. Challis, R.C., et al., Systemic AAV vectors for widespread and targeted gene delivery in rodents. *Nat Protoc*, 2019. **14**(2): p. 379–414.
14. Yuasa, K., et al., Adeno-associated virus vector-mediated gene transfer into dystrophin-deficient skeletal muscles evokes enhanced immune response against the transgene product. *Gene Ther*, 2002. **9**(23): p. 1576–88.
15. Stieger, K., et al., Long-term doxycycline-regulated transgene expression in the retina of nonhuman primates following subretinal injection of recombinant AAV vectors. *Mol Ther*, 2006. **13**(5): p. 967–75.
16. Vanrell, L., et al., Development of a liver-specific Tet-on inducible system for AAV vectors and its application in the treatment of liver cancer. *Mol Ther*, 2011. **19**(7): p. 1245–53.
17. Dogbevia, G.K., et al., Flexible, AAV-equipped Genetic Modules for Inducible Control of Gene Expression in Mammalian Brain. *Mol Ther Nucleic Acids*, 2016. **5**: p. e309.
18. Sohn, J., et al., A Single Vector Platform for High-Level Gene Transduction of Central Neurons: Adeno-Associated Virus Vector Equipped with the Tet-Off System. *PLoS One*, 2017. **12**(1): p. e0169611.
19. Reid, C.A., et al., Development of an inducible anti-VEGF rAAV gene therapy strategy for the treatment of wet AMD. *Sci Rep*, 2018. **8**(1): p. 11763.
20. Monteys, A.M., et al., Regulated control of gene therapies by drug-induced splicing. *Nature*, 2021. **596**(7871): p. 291–295.
21. Chan, K.Y., et al., Engineered AAVs for efficient noninvasive gene delivery to the central and peripheral nervous systems. *Nat Neurosci*, 2017. **20**(8): p. 1172–1179.
22. Xiong, W., et al., NRF2 promotes neuronal survival in neurodegeneration and acute nerve damage. *J Clin Invest*, 2015. **125**(4): p. 1433–45.
23. Yeh, H.W., et al., Red-shifted luciferase-luciferin pairs for enhanced bioluminescence imaging. *Nat Methods*, 2017. **14**(10): p. 971–974.
24. Li, X., et al., Synthetic muscle promoters: activities exceeding naturally occurring regulatory sequences. *Nat Biotechnol*, 1999. **17**(3): p. 241–5.
25. Lundstrom, K., *Viral Vectors in Gene Therapy. Diseases*, 2018. **6**(2).
26. Cabanes-Creus, M., et al., Restoring the natural tropism of AAV2 vectors for human liver. *Sci Transl Med*, 2020. **12**(560).
27. Carneiro, A., et al., Novel Lung Tropic Adeno-Associated Virus Capsids for Therapeutic Gene Delivery. *Hum Gene Ther*, 2020. **31**(17–18): p. 996–1009.
28. Charsar, B.A., et al., AAV2-BDNF promotes respiratory axon plasticity and recovery of diaphragm function following spinal cord injury. *FASEB J*, 2019. **33**(12): p. 13775–13793.
29. George, L.A., et al., Long-Term Follow-Up of the First in Human Intravascular Delivery of AAV for Gene Transfer: AAV2-hFIX16 for Severe Hemophilia B. *Mol Ther*, 2020. **28**(9): p. 2073–2082.
30. Gross, S.K., et al., Focal and dose-dependent neuroprotection in ALS mice following AAV2-neurturin delivery. *Exp Neurol*, 2020. **323**: p. 113091.
31. Qiao, C., et al., Adeno-associated virus serotype 6 capsid tyrosine-to-phenylalanine mutations improve gene transfer to skeletal muscle. *Hum Gene Ther*, 2010. **21**(10): p. 1343–8.

32. Riaz, M., et al., Differential myofiber-type transduction preference of adeno-associated virus serotypes 6 and 9. *Skelet Muscle*, 2015. **5**: p. 37.
33. Pattali, R., Y. Mou, and X.J. Li, AAV9 Vector: a Novel modality in gene therapy for spinal muscular atrophy. *Gene Ther*, 2019. **26**(7–8): p. 287–295.
34. Saraiva, J., R.J. Nobre, and L. Pereira de Almeida, Gene therapy for the CNS using AAVs: The impact of systemic delivery by AAV9. *J Control Release*, 2016. **241**: p. 94–109.
35. Zhou, X., et al., Optimization of the Tet-On system for regulated gene expression through viral evolution. *Gene Ther*, 2006. **13**(19): p. 1382–90.
36. Hastie, E. and R.J. Samulski, Adeno-associated virus at 50: a golden anniversary of discovery, research, and gene therapy success--a personal perspective. *Hum Gene Ther*, 2015. **26**(5): p. 257–65.
37. Wu, Z., A. Asokan, and R.J. Samulski, Adeno-associated virus serotypes: vector toolkit for human gene therapy. *Mol Ther*, 2006. **14**(3): p. 316–27.
38. Maguire, A.M., et al., Safety and efficacy of gene transfer for Leber's congenital amaurosis. *N Engl J Med*, 2008. **358**(21): p. 2240–8.
39. Zincarelli, C., et al., Analysis of AAV serotypes 1–9 mediated gene expression and tropism in mice after systemic injection. *Mol Ther*, 2008. **16**(6): p. 1073–80.
40. Gao, G., et al., Transendocardial delivery of AAV6 results in highly efficient and global cardiac gene transfer in rhesus macaques. *Hum Gene Ther*, 2011. **22**(8): p. 979–84.
41. Ji, G., et al., Effect of AAV9-hIGF-1 on inflammatory reaction in mdx mice and its mechanism. *Am J Transl Res*, 2020. **12**(8): p. 4488–4497.
42. Kolwicz, S.C., Jr., et al., AAV6-mediated Cardiac-specific Overexpression of Ribonucleotide Reductase Enhances Myocardial Contractility. *Mol Ther*, 2016. **24**(2): p. 240–250.
43. Moulay, G., et al., Soluble TNF-alpha receptor secretion from healthy or dystrophic mice after AAV6-mediated muscle gene transfer. *Gene Ther*, 2010. **17**(11): p. 1400–10.
44. Hermiston, T.W., et al., Identification and characterization of the human cytomegalovirus immediate-early region 2 gene that stimulates gene expression from an inducible promoter. *J Virol*, 1987. **61**(10): p. 3214–21.
45. Thomsen, D.R., et al., Promoter-regulatory region of the major immediate early gene of human cytomegalovirus. *Proc Natl Acad Sci U S A*, 1984. **81**(3): p. 659–63.
46. Harms, J.S. and G.A. Splitter, Interferon-gamma inhibits transgene expression driven by SV40 or CMV promoters but augments expression driven by the mammalian MHC I promoter. *Hum Gene Ther*, 1995. **6**(10): p. 1291–7.
47. Hartigan-O'Connor, D., et al., Immune evasion by muscle-specific gene expression in dystrophic muscle. *Mol Ther*, 2001. **4**(6): p. 525–33.
48. Wang, B., et al., Construction and analysis of compact muscle-specific promoters for AAV vectors. *Gene Ther*, 2008. **15**(22): p. 1489–99.
49. Sanftner, L.H.M., et al., Recombinant AAV-mediated delivery of a tet-inducible reporter gene to the rat retina. *Molecular Therapy*, 2001. **3**(5): p. 688–696.
50. Chtarto, A., et al., Tetracycline-inducible transgene expression mediated by a single AAV vector. *Gene Ther*, 2003. **10**(1): p. 84–94.
51. Wang, J.J., et al., Doxycycline-regulated co-expression of GDNF and TH in PC12 cells. *Neurosci Lett*, 2006. **401**(1–2): p. 142–5.
52. Folliot, S., et al., Sustained tetracycline-regulated transgene expression in vivo in rat retinal ganglion cells using a single type 2 adeno-associated viral vector. *J Gene Med*, 2003. **5**(6): p. 493–501.
53. Li, Z.B., et al., Recombinant AAV-mediated HSVtk gene transfer with direct intratumoral injections and Tet-On regulation for implanted human breast cancer. *BMC Cancer*, 2006. **6**: p. 66.
54. Ziegler, T., et al., Steerable Induction of the Thymosin beta4/MRTF-A Pathway via AAV-Based Overexpression Induces Therapeutic Neovascularization. *Hum Gene Ther*, 2017.
55. Liu, Y., et al., Protection Against Aminoglycoside-induced Ototoxicity by Regulated AAV Vector-mediated GDNF Gene Transfer Into the Cochlea. *Mol Ther*, 2008. **16**(3): p. 474–480.

- 
56. Kiyota, T., et al., AAV2/1 CD74 Gene Transfer Reduces beta-amyloidosis and Improves Learning and Memory in a Mouse Model of Alzheimer's Disease. *Mol Ther*, 2015. **23**(11): p. 1712–1721.
  57. Gafni, Y., et al., Gene therapy platform for bone regeneration using an exogenously regulated, AAV-2-based gene expression system. *Mol Ther*, 2004. **9**(4): p. 587–95.
  58. Sweeney, C.G., et al., Conditional, inducible gene silencing in dopamine neurons reveals a sex-specific role for Rit2 GTPase in acute cocaine response and striatal function. *Neuropsychopharmacology*, 2020. **45**(2): p. 384–393.
  59. de Solis, C.A., et al., The Development of a Viral Mediated CRISPR/Cas9 System with Doxycycline Dependent gRNA Expression for Inducible In vitro and In vivo Genome Editing. *Front Mol Neurosci*, 2016. **9**: p. 70.
  60. Watakabe, A., et al., Simultaneous visualization of extrinsic and intrinsic axon collaterals in Golgi-like detail for mouse corticothalamic and corticocortical cells: a double viral infection method. *Front Neural Circuits*, 2014. **8**: p. 110.
  61. Guilbaud, M., et al., Five Years of Successful Inducible Transgene Expression Following Locoregional Adeno-Associated Virus Delivery in Nonhuman Primates with No Detectable Immunity. *Hum Gene Ther*, 2019. **30**(7): p. 802–813.
  62. Gao, G., et al., Biology of AAV serotype vectors in liver-directed gene transfer to nonhuman primates. *Mol Ther*, 2006. **13**(1): p. 77–87.
  63. Pulicherla, N., et al., Engineering liver-detargeted AAV9 vectors for cardiac and musculoskeletal gene transfer. *Mol Ther*, 2011. **19**(6): p. 1070–8.
  64. Wang, D. and G. Gao, Taking a Hint from Structural Biology: To Better Understand AAV Transport across the BBB. *Mol Ther*, 2018. **26**(2): p. 336–338.
  65. Tabebordbar, M., et al., Directed evolution of a family of AAV capsid variants enabling potent muscle-directed gene delivery across species. *Cell*, 2021. **184**(19): p. 4919–4938 e22.



SUPPLEMENTRY MATERIALS

Adult mice were injected with  $1 \times 10^{14}$  vg/kg virus via retro-orbital administration. Images were taken 1 month after viral injection via *in vivo* imaging system (IVIS). Diphenylterazine (DTZ) were injected 5 minutes before imaging. (A) without virus injection; (B) with virus injection.

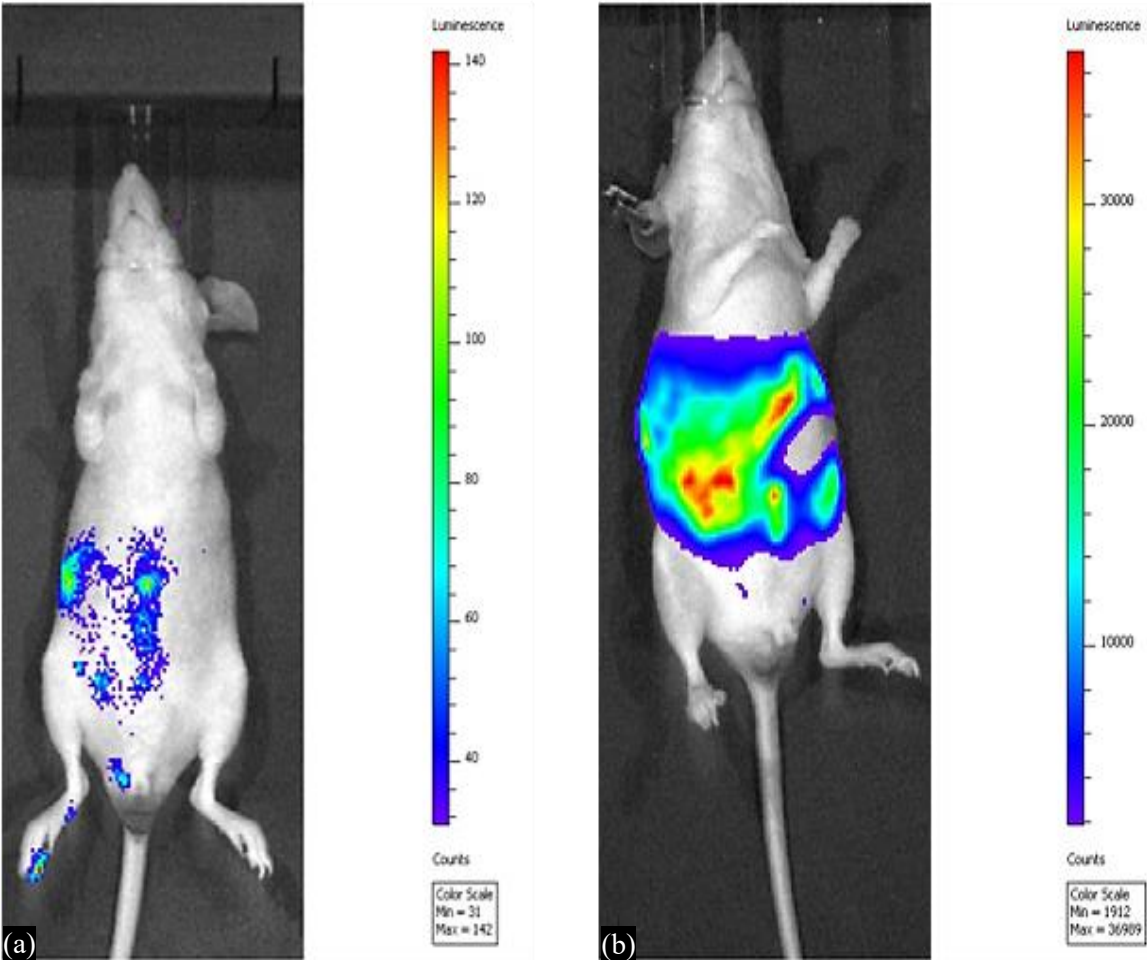
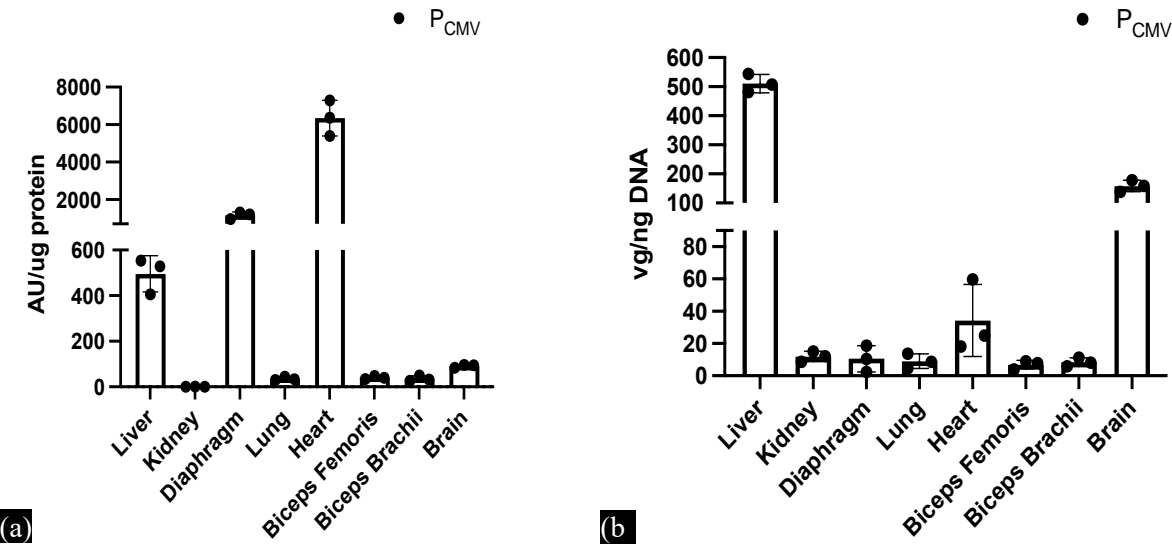
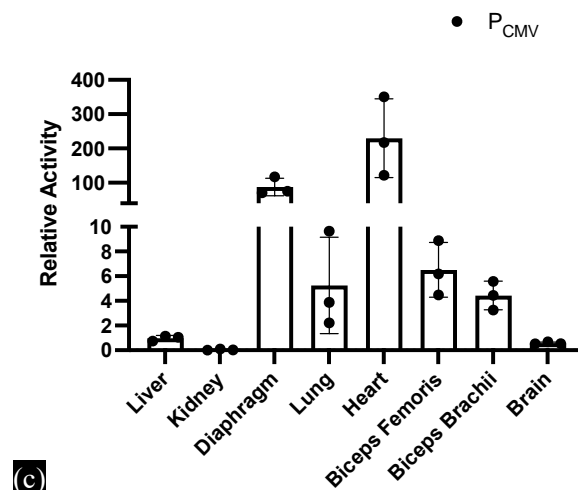


Figure S1. (a, b) Bioluminescence imaging of hairless mice after AAV9-PCMV-teLuc IV viral injection.





**Figure S2.** (a–c) Tissue Analysis of Luciferase Activity Induced by AAV9- $P_{CMV}$ -teLuc Vectors.

Heart, lung, diaphragm, liver, kidney, biceps femoris, biceps brachii muscles, and brain tissue were collected one month after virus injection. (A) Luciferase activity of tissue sample of AAV9- $P_{CMV}$ -teLuc injection. Luciferase activities were assayed with substrate DTZ. Data are mean  $\pm$  SD,  $n=3$  each group. (B) Virus gene copy number analyzed by qPCR. Data are mean  $\pm$  SD. (C) Virus gene relative activity of animal tissue after AAV9- $P_{CMV}$ -teLuc injection. Data are mean  $\pm$  SD. Virus gene relative activities were calculated as the bioluminescence from the tissue luciferase assay normalized by viral genome copy number in of same piece of tissue.